DOI: 10.18462/iir.gl2022.0237

Experimental investigation on integrated two-stage evaporators for CO_2 heat-pump chillers

Armin HAFNER[(*a)], Mihir Mouchum HAZARIKA[(a)], Federico LECHI[(b)], Alvaro ZORZIN[(b)], Ángel Álvarez PARDIÑAS[(c)], Krzysztof BANASIAK[(a)]

[(a)] Norwegian University of Science and Technology, *armin.hafner@ntnu.no

[(b)]Business Unit Brazed & Fusion Bonded Heat Exchangers, Alfa Laval Spa, Italy

[(c)]Thermal Energy, SINTEF Energy Research, Trondheim

ABSTRACT

In this experimental study the performance of novel compact evaporator configuration was investigated. What makes this evaporator configuration unique is the integration of a gravity-fed/ self-circulation evaporator loop on one side of a plate heat exchanger (pre-cooling the secondary flow) and an ejector-assisted circulation loop on the other side (after-cooling the secondary flow). The secondary loop is internally connected, which means that larger temperature differences can be obtained with less connection work and space required, compared to previous heat exchanger models.

Current CO_2 heat-pump chillers available on the market utilize two evaporators to achieve high energy efficiency values. Space saving of the new compact design is a desired solution from vendors. When using this new concept, only one 'three-circuit' brazed heat exchanger is needed. The experimental campaign proofed that an ejector integration enables the two-stage evaporation configuration which significantly elevates the compressor suction pressure and improves the overall system performance. These systems can be applied in several market sectors including industrial chillers with high-capacity demands, where the secondary fluid is cooled even below 0°C.

Keywords: Carbon Dioxide, two stage evaporation, ejector, chiller

1. INTRODUCTION

Flooded evaporators, i.e. without and active superheating part, are regarded as simple and effective modification incorporated in a refrigeration system to enhance the performance. These evaporators are designed to utilize the entire surface for evaporation only, therefore the internal surface is not completely dry. The higher the presence of liquid at the cooling coil surface, the higher is the heat transfer coefficient which leads to better overall heat transfer rate. Lorentzen (1968) presented the benefits of using flooded evaporators over dry expansion evaporators. It was reported that the average efficiency of dry expansion evaporators is less than half of the efficiency of flooded evaporators. Improved heat transfer rates in flooded evaporators give the opportunity to operate the evaporator at a relatively higher evaporation temperature. Karampour and Sawalha (2018) presented that the evaporation temperature can be increased by 3-4 K in CO_2 units, when applying flooded evaporators as compared to dry expansion evaporators. There is more research available

This is the accepted version of a paper published at GL2022
http://dx.doi.org/10.18462/iir.gl2022.0237

in the literature that presents different methods on how to implement flooded evaporators in CO_2 system. Minetto et al. (2014) implemented a method in a CO_2 system where the ejector was utilized to operate multiple evaporators on flooded mode arranged in parallel. Hafner (2018) and Tosato et al. (2020) presented a new method with two evaporators where one evaporator was operated on gravity-fed mode and the other was operated on ejector supported mode. They reported the benefits of using this new configuration in CO_2 heat pumps.

The present study is carried out to explore the possibilities of using flooded evaporator in a CO_2 heat-pump chiller to enhance its performance. A novel concept is proposed in this study in which a two-stage evaporator configuration is utilized. First stage of this evaporator operates on gravity-fed mode, as shown in Figure 1, while the second stage operates on ejector supported mode. Both stages of the heat exchanger are joined together in a sandwiched fashion to design the novel and compact configuration. The passage for the secondary fluid is internally connected within the heat exchanger in such a way that the fluid first passes through the gravity-fed evaporator and then through the ejector supported evaporator. The evaporation pressure is different for the two stages of the heat exchanger. The first stage, i.e., the gravity-fed evaporator operates at the separator pressure = suction pressure of the compressor, while the second stage, i.e., the ejector supported evaporator operates at the suction pressure of the ejector utilizing the available expansion work. Thus, it is possible to achieve a pressure difference of around 5 bar between the two stages at high side pressures above 80 bar and expansion device inlet temperatures above 25°C. This two-stage design enables to generate a larger temperature glide on the secondary fluid side. In addition, it is possible to enhance the overall system performance of the system as the cooling capacity is shared between two stages of the heat exchanger and the suction pressure of compressor can be significantly elevated by utilizing the ejector. In the present work, a prototype of this novel two-stage evaporator is implemented in a CO_2 test facility at NTNU/SINTEF. Experiments are carried out to gain and analyze the initial performance of this two-stage evaporator under different operation conditions: e.g., evaporation pressure, secondary fluid temperature, and secondary fluid flowrate. The initial steady-state results are presented in this paper.

2. WORKING PRINCIPLE

Figure 1 shows the schematic of self-circulation loop and ejector-assisted circulation loop within the two-stage evaporator. This evaporator is a two-stage plate heat exchanger and is designed in such a way that the first stage (right hand part in Figure 1) of the heat exchanger is a self-circulation loop (gravity driven). The second stage (left hand part in Figure 1) of the heat exchanger is connected to the suction port of the ejector, which acts as a pre-compression stage. The secondary fluid path is internally connected within the heat exchanger. The pre-cooling of secondary fluid is carried out in the self-circulation loop at elevated evaporation pressure (equal to receiver and compressor suction pressure) while the after-cooling of secondary fluid is carried out in the ejector-assisted loop, at significantly lower evaporation temperatures. The refrigerant flowrate and pressure level in the ejector-assisted loop depends on the performance of the ejector and the available expansion work. The refrigerant flowrate through the self-circulation loop depends mainly on the density differences in that loop. This density difference arises as the heat exchange process takes place in the heat exchanger. The static liquid height ‘H’ acts as a prime mover to overcome all the pressure resistances present in the self-circulation loop and maintain the certain flowrate.

This is the accepted version of a paper published at GL2022
http://dx.doi.org/10.18462/iir.gl2022.0237

This two-stage evaporator is operated on flooded mode with liquid refrigerant supplied to it from the separator. The target is to get relative high vapor fractions (≈0.8) at the refrigerant exit of the two-stage evaporator for both loops. In the self-circulation loop, the refrigerant downstream of the evaporator returns directly back to the separator. In the ejector-assisted loop, the refrigerant downstream of the evaporator enters the ejector through the suction nozzle. In the ejector, the suction flow (~ 50% of the compressor flowrate) is mixed with the motive flow (100% of flowrate). The mixed flow downstream of the ejector enters the separator. In the separator, liquid and vapor are separated. Liquid refrigerant is utilized for the evaporators, while the vapor is sucked by the compressor and thereafter distributed to the heat rejection devices, i.e., the gas cooler(s). The refrigerant leaving the gas cooler is sent to the motive nozzle of the ejector.

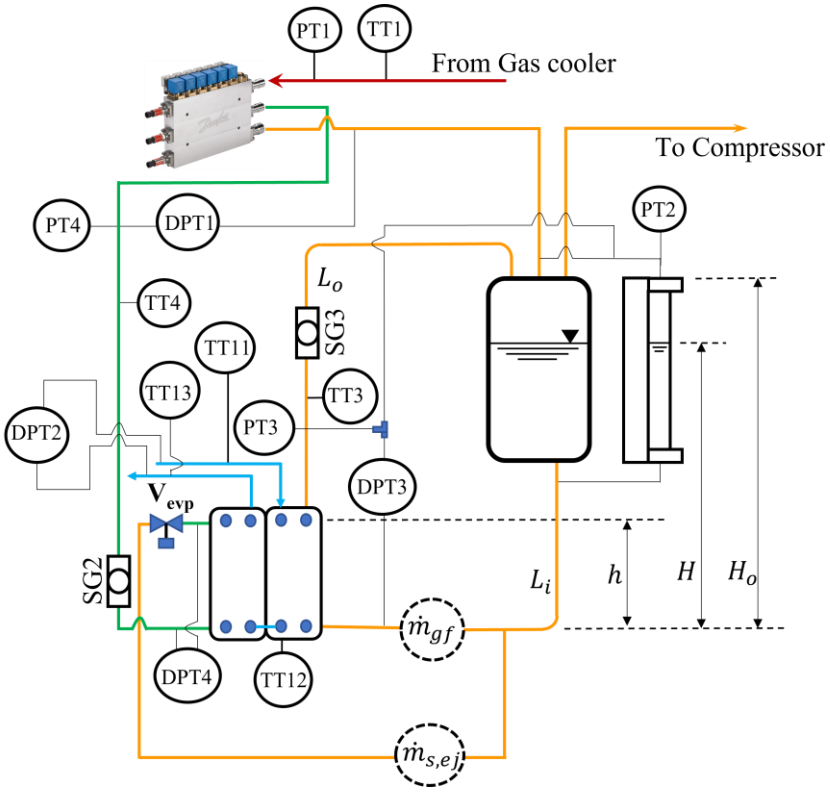

Figure 1: Schematic of self-circulation loop and ejector-assisted loop with two-stage evaporator

Table 1: List of sensors

Sensor	Location	Sensor	Location
PT1	Ejector motive pressure	TT1	Ejector motive temperature
PT2	Separator pressure	TT3	Gravity-fed evaporator outlet temperature
PT3	Gravity-fed evaporator outlet pressure	TT4	Ejector supported evaporator outlet temperature

This is the accepted version of a paper published at GL2022
http://dx.doi.org/10.18462/iir.gl2022.0237

PT4	Ejector supported evaporator outlet pressure	TT11	Water inlet temperature
DPT1	Pressure lift of ejector	TT12	Water temperature at intermediate section of two-stage evaporator
DPT2	Water-side pressure drop across the two-stage evaporator	TT13	Water outlet temperature
DPT3	CO_2-side pressure drop across gravity-fed evaporator	$\dot{m}_{gf}$	Self-circulation CO_2 mass flowrate in gravity-fed loop
DPT4	CO_2-side pressure drop across ejector supported evaporator	$\dot{m}_{s,ej}$	Suction CO_2 mass flowrate in ejector supported loop

3. EXPERIMENTAL PROCEDURE

Figure 2: Picture of the CO_2 facility at NTNU/SINTEF with the two-stage evaporator on the lower left-hand side.

The prototype of the two-stage evaporator is installed at the test-facility at the NTNU/SINTEF research laboratory. This prototype heat exchanger is designed by Alfa Laval. It is a brazed plate heat exchanger with 80 plates (40 plates for each stage, gravity-fed and ejector supported). The length and width of each plate are 420 mm and 155 mm respectively. Figure 2 shows the image of the unit with the two-stage evaporator. The measuring instruments are installed at the suitable locations, as indicated in Figure 1, in the test set-up to measure pressure, temperature, differential pressure, refrigerant mass flowrate, and secondary fluid mass flowrate. The list of all sensors is shown in Table 1. Experiments are carried out to obtain and analyse steady-state results under different conditions. The following parameters have been varied during this initial campaign:

This is the accepted version of a paper published at GL2022
http://dx.doi.org/10.18462/iir.gl2022.0237

evaporation pressure, secondary fluid temperature, and secondary fluid mass flowrate. The initial test matrix is shown in Table 2.

Table 2: Initial test matrix and achieved water temperature levels

Sl. No.	Water inlet temperature (°C)	Water temperature at intermediate section (°C)	Water outlet temperature (°C)	Water flowrate (kg. min^{-1})	Evaporation pressure at gravity-fed evaporator (bar)	Evaporation pressure at ejector supported evaporator (bar)
1	20.0	14.16	7.93	24	42.2	38
2	17.5	11.97	6.96	24	42.2	38
3	15.0	9.78	5.95	24	42.3	38
4	13.5	8.81	5.50	24	42.2	38
5	12.0	8.35	5.25	24	42.2	38
6	20.0	14.74	10.14	24	45.0	41
7	17.5	12.50	9.09	24	45.0	41
8	16.5	11.79	8.74	24	45.0	41
9	15.0	11.21	8.42	24	45.0	41
10	20.0	12.69	6.96	18	42.4	38
11	20.0	11.57	6.15	16	42.2	38
12	20.0	9.49	5.21	12	42.2	38
13	15.0	8.80	5.25	18	42.2	38
14	15.0	8.12	4.76	16	42.2	38
15	15.0	7.87	4.23	12	42.0	38
16	12.0	8.14	4.90	18	42.2	38
17	12.0	7.93	4.69	16	42.2	38
18	12.0	7.93	4.56	12	42.2	38

(These tests are carried out maintaining fixed pressure and temperature of 80 bar and 35 °C respectively at the inlet of ejector motive nozzle. The opening degree of expansion valve in the ejector supported loop is maintained at 25 %.)

4. RESULTS AND DISCUSSION

This section presents the experimental results for the novel two-stage evaporator. During the experimental campaign, the water inlet temperature is varied from 12 °C to 20 °C, while the water flowrate is varied from 12 kg/min to 24 kg/min. Figure 3 shows the cooling capacity of the gravity-fed evaporator with various water flowrates and water inlet temperatures. As expected, it can be observed that the effect of the water flowrate on the cooling capacity is less dominant than the effect of the water inlet temperature. As the water inlet temperature increases, the cooling capacity increases sharply. However, the cooling capacity increase is moderate when adjusting the water flowrates. Figure 4 shows the cooling capacity of ejector supported evaporator. Its performance

This is the accepted version of a paper published at GL2022
http://dx.doi.org/10.18462/iir.gl2022.0237

depends on the performance of gravity-fed evaporator. To analyse the coupled effects of gravity-fed evaporator and ejector supported evaporator, the approach temperatures (difference between the water outlet temperature and the evaporation temperature) are plotted in Figures 5 & 6. The temperature glide on the waterside are plotted in Figures 7 & 8. As the water inlet temperature increases, the approach temperature increases for the gravity-fed evaporator (Figure 5). Cooling

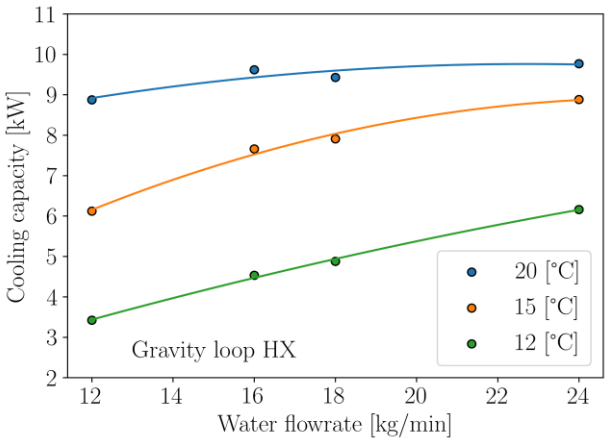

Figure 3: Cooling capacity of gravity-fed evaporator with water flowrate at 42 bar evaporation pressure

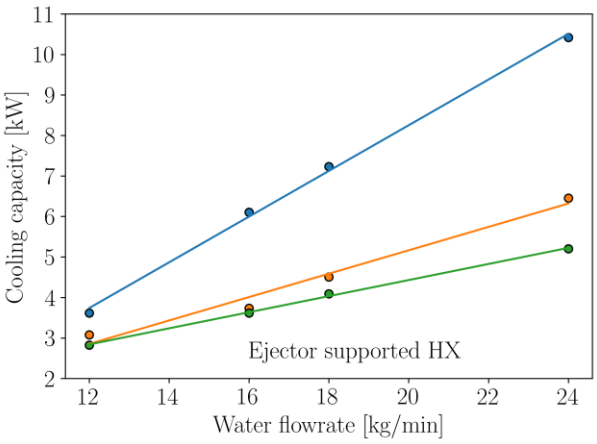

Figure 4: Cooling capacity of ejector supported evaporator with water flowrate at 38 bar evap. pressure

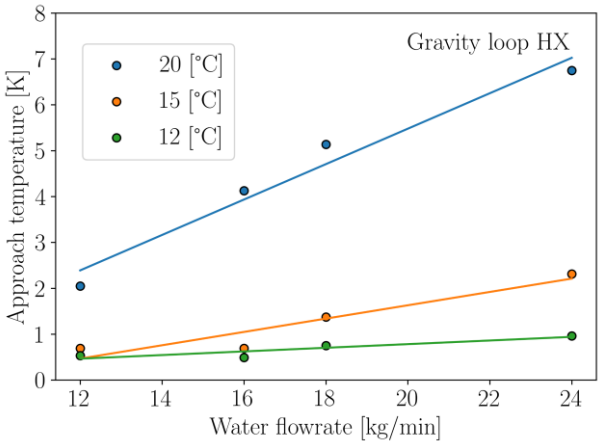

Figure 5: Approach temperature for gravity-fed evaporator with water flowrate at 42 bar evap. pressure

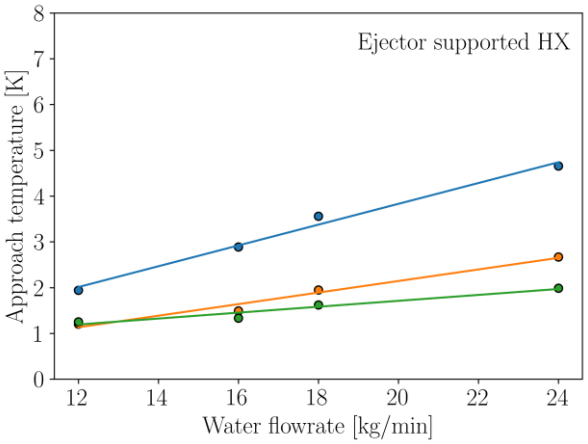

Figure 6: Approach temperature for ejector supported evaporator with water flowrate at 38 bar evap. pressure

capacity also increases (Figure 3). At low water flowrates and high cooling capacities, there is a larger temperature drop on the waterside in the first (gravity-fed) evaporator (Figure 7). This leads to low temperature difference in between refrigerant and water at the entrance of the ejector-supported evaporator. Hence, the cooling capacity is very low for ejector supported evaporator (Figure 4) at low water flowrates. However, as the water flowrate is increased, water-side temperature drop decreases for gravity-fed evaporator (Figure 7). This leads to high temperature difference in between refrigerant and water at the entrance of the ejector-supported evaporator. Hence, cooling capacity increases for the ejector supported evaporator at high water flowrate (Figure 4). This means at high load conditions this configuration can provide cooling with a share

This is the accepted version of a paper published at GL2022
http://dx.doi.org/10.18462/iir.gl2022.0237

of 50/50 in both heat exchangers (high water inlet temperature & high water flowrate). Logarithmic mean temperature differences (LMTDs) for gravity-fed evaporator and ejector supported evaporator are plotted in Figures 9 and 10. Higher the water inlet temperature, higher is the difference in temperature between refrigerant and water. Hence, LMTD is large for high water inlet temperature.

As an example, it is observed that for a water flowrate of 24 kg/min, and water inlet temperature of 15 °C, the water-side temperature drop is 5.2 K through the gravity-fed evaporator and additional 3.8 K via the ejector supported evaporator.

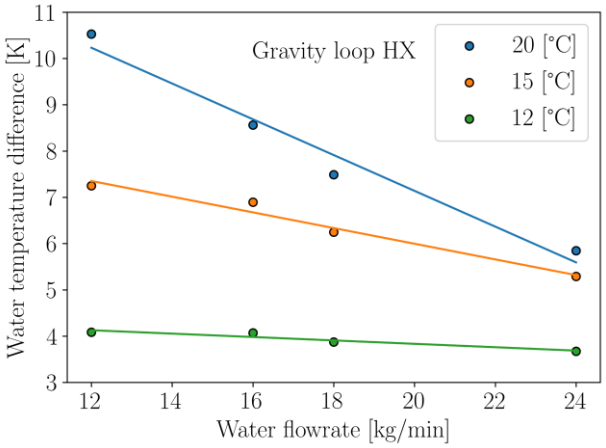

Figure 7: Temperature drop on waterside for gravity-fed evaporator with water flowrate at 42 bar evap. pressure

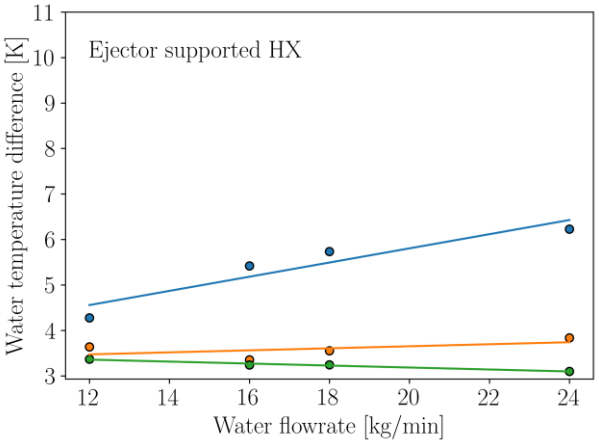

Figure 8: Temperature drop on waterside for ejector supported evaporator with water flowrate at 38 bar evap. pressure
(Water inlet temperature, see Table 2)

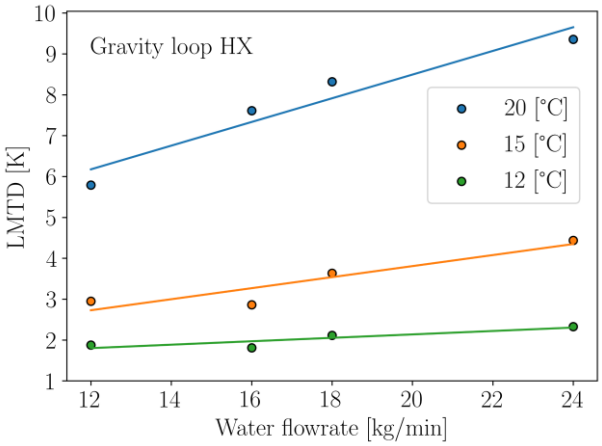

Figure 9: LMTD for gravity-fed evaporator with water flowrate at 42 bar evap. pressure

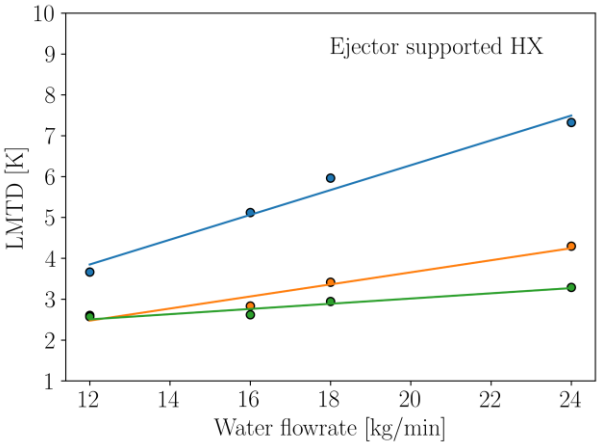

Figure 10: LMTD for ejector supported evaporator with water flowrate at 38 bar evap. pressure

To analyse the effects of water inlet temperature on the two-stage evaporator at different evaporation pressures, experiments were carried out and results are presented here (at a water flowrate of 24 kg/min). The ejector supported evaporator is maintained at evaporation pressure of 38 bar and 41 bar. During the experiments, the pressure lift in the ejector is found to be

This is the accepted version of a paper published at GL2022
http://dx.doi.org/10.18462/iir.gl2022.0237

approximately 4 bar for all operating conditions. Hence the evaporation pressure is approximately 42 bar and 45 bar in the gravity-fed evaporator.

Figure 11 shows the cooling capacity of gravity-fed evaporator, while Figure 12 shows the cooling capacity of ejector supported evaporator. The performance of ejector supported evaporator depends on the performance of gravity-fed evaporator. To analyse the coupled effects of gravity-fed evaporator and ejector supported evaporator, approach temperatures are plotted in Figures 13 & 14, while water-side temperature drops are plotted in Figures 15 & 16. As the water inlet temperature increases, the approach temperature increases for gravity-fed evaporator (Figure 13). Cooling capacity also increases. It is observed that cooling capacity first increases sharply and then

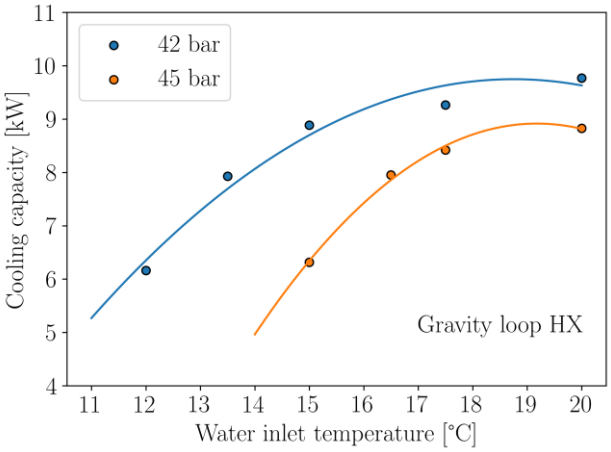

Figure 11: Cooling capacity of gravity-fed evaporator with water inlet temperature for water flowrate of 24 kg/min

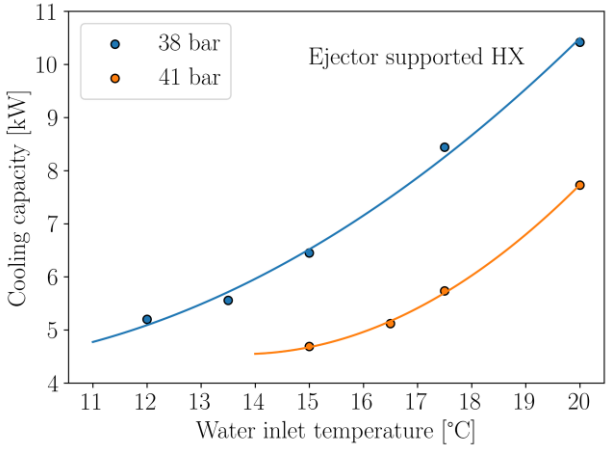

Figure 12: Cooling capacity of ejector supported evaporator with water inlet temperature for water flowrate of 24 kg/min

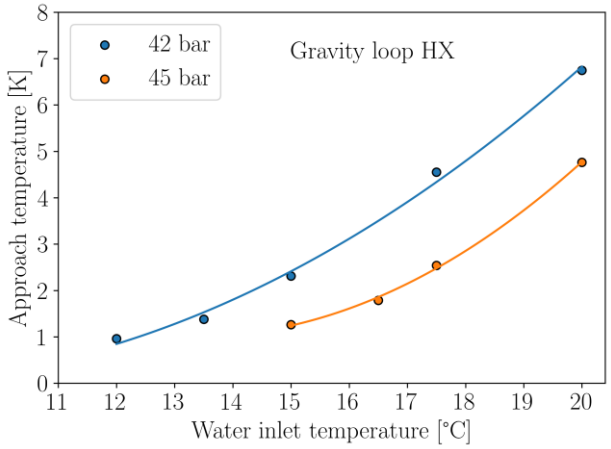

Figure 13: Approach temperature for gravity-fed evaporator with water inlet temperature for water flowrate of 24 kg/min

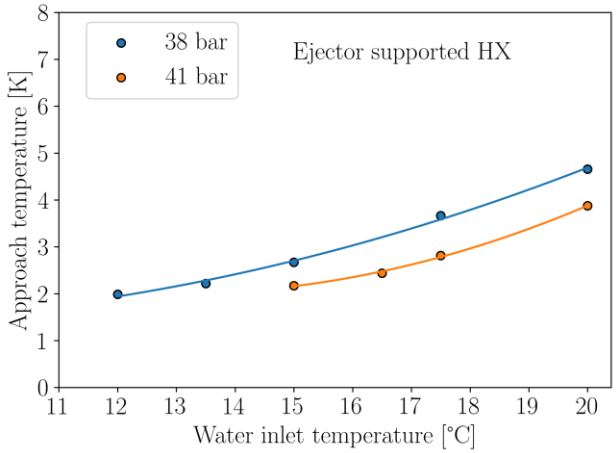

Figure 14: Approach temperature for ejector supported evaporator with water inlet temperature for water flowrate of 24 kg/min

becomes stagnant (Figure 11) with an increase in water inlet temperature. This is due to the shape of the isotherm close to saturated vapor state. When the exit state of evaporator is either within two-phase region or close to saturated vapor state, for a unit change in water temperature, the

This is the accepted version of a paper published at GL2022
http://dx.doi.org/10.18462/iir.gl2022.0237

change in specific enthalpy difference is large. However, if the exit state of evaporator is far from the saturated vapor state, the change in specific enthalpy difference is small for a unit change in temperature. Hence, the cooling capacity of gravity-fed evaporator first increases sharply and then becomes stagnant. As a result, the temperature drop on water-side shows a similar trend (Figure 15) through the gravity-fed evaporator. When the water-side temperature drop is large in gravity-fed evaporator, the temperature difference between water and refrigerant at the entrance of ejector supported evaporator becomes low and vice versa. Cooling capacity of ejector supported evaporator increases (Figure 12) for large temperature difference at the entrance. LMTDs for gravity-fed evaporator and ejector supported evaporator are plotted in Figures 17 and 18. Higher the water inlet temperature, higher is the difference in temperature between refrigerant and water. Hence, LMTD increases with an increase in water inlet temperature.

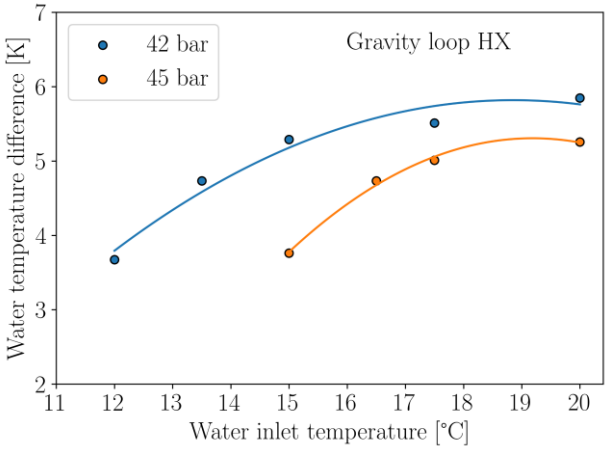

Figure 15: Temperature drop on waterside for gravity-fed evaporator with water inlet temperature for water flowrate of 24 kg/min

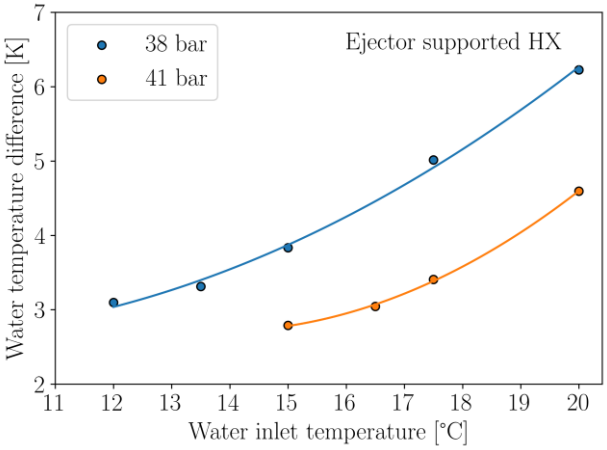

Figure 16: Temperature drop on waterside for ejector supported evaporator with water inlet temperature for water flowrate of 24 kg/min

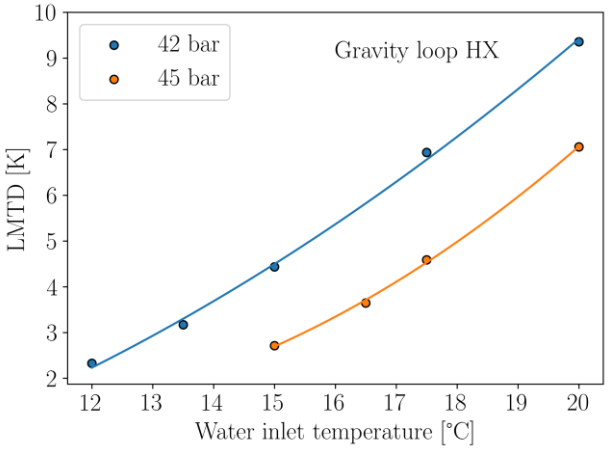

Figure 17: LMTD for gravity-fed evaporator with water inlet temperature for water flowrate of 24 kg/min

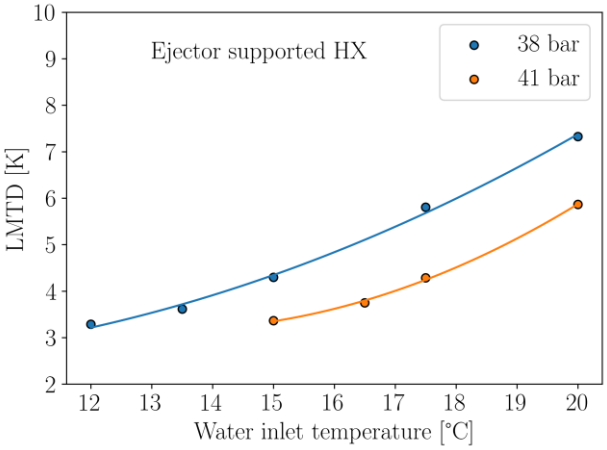

Figure 18: LMTD for ejector supported evaporator with water inlet temperature for water flowrate of 24 kg/min

This is the accepted version of a paper published at GL2022
http://dx.doi.org/10.18462/iir.gl2022.0237

5. CONCLUSIONS

This study presents initial performance results of a novel and compact two-stage evaporator configuration designed in such a way that the first stage of the heat exchanger operates on gravity-fed mode, while the second stage operates on ejector supported mode. This configuration gives the opportunity to achieve a large temperature glide on the secondary fluid side, as the two stages of the heat exchanger are operated at different evaporation pressure/temperature levels. Experimental results show that for low water flowrates, the water-side temperature drop is very large on gravity-fed evaporator, i.e. providing the main capacity, representing part load operation. This leads to low temperature difference in between refrigerant and water at the entrance of the ejector supported evaporator and hence cooling capacity is low for this evaporator. However, as the water flowrate increases or the cooling demand, the water-side temperature drop decreases on gravity-fed evaporator. This leads to high temperature difference at the entrance of the ejector supported evaporator and hence the cooling capacity also increases. It is observed that for a water mass flowrate of 24 kg/min, and water inlet temperature of 15 °C, the waterside temperature drop is 5.2 K on gravity-fed evaporator and 3.8 K on ejector supported evaporator. The experimental results also show that the effect of water inlet temperature is more dominant on the cooling capacity as compared to water flowrate.

Besides, this two-stage heat exchanger is designed in such a way that both stages are operated on a non-superheated mode on the refrigerant side. This enhances the heat transfer coefficient significantly. Improved heat transfer rate gives the possibility to design this heat exchanger compact with high volumetric capacity. In addition, there is an improvement in the overall performance as the cooling capacity is shared between two stages of the heat exchanger and the compressor suction pressure is elevated by utilizing the expansion work with an ejector.

Installation space is significantly reduced as only two connections are required on the secondary fluid side.

ACKNOWLEDGEMENTS

The authors would like to acknowledge the support received from national research projects funded by the Research Council of Norway, i.e. the CoolFish project, FME-HighEFF, the Heat-Jet project. In addition: AlfaLaval for providing the prototype heat exchanger.

This is the accepted version of a paper published at GL2022
http://dx.doi.org/10.18462/iir.gl2022.0237

REFERENCE

Hafner, A. 2018. Latest CO_2 refrigeration trends, Proceedings of the Atmosphere Europe event Lago di Garda, Italy, 19-21.11.2018

Karampour, M., Sawalha, S., 2018. State-of-the-art integrated CO_2 refrigeration system for supermarkets: A comparative analysis. Int. J. Refrig. 86, 239–257.

Lorentzen, G., 1968. Evaporator design and liquid feed regulation. Int. J. Refrig. (November December).

Minetto, S., Brignoli, R., Zilio, C., Marinetti, S., 2014. Experimental analysis of a new method for overfeeding multiple evaporators in refrigeration systems. Int. J. Refrig. 38, 1–9.

Tosato, G., Girotto, S., Minetto, S., Rossetti, A., Marinetti, S., 2020. An integrated CO_2 unit for heating, cooling and DHW installed in a hotel. Data from the field. J. Phys. Conf. Ser. 1599.

Open access to applied data

Hafner, Armin; Hazarika, Mihir Mouchum; Lechi, Federico; Zorzin, Alvaro; Pardiñas, Ángel Álvarez; Banasiak, Krzysztof, 2022, "Experimental investigation on integrated two-stage evaporators for CO2 heat-pump chillers", https://doi.org/10.18710/BSOG2S

This is the accepted version of a paper published at GL2022
http://dx.doi.org/10.18462/iir.gl2022.0237